Incoherent Inelastic Neutron Scattering, Infrared, Raman, and X-ray Diffraction Studies of Pentacarbonylmethylmanganese, $Mn(CO)_5CH_3$

Mark A. Andrews,*[1a] J. Eckert,[1d] J. A. Goldstone,[1d] Laurence Passell,[1b] and Basil Swanson[1c]

Contribution from the Departments of Chemistry and Physics, Brookhaven National Laboratory, Upton, New York 11973, and the Departments of Chemistry and Physics, Los Alamos National Laboratory, Los Alamos, New Mexico 87545. *Received May 3, 1982*

Abstract: Vibrational spectra for the prototype transition-metal alkyl complex pentacarbonylmethylmanganese have been obtained by incoherent inelastic neutron scattering (0–3200 cm^{-1}, 0–400 meV) and by infrared (400–4800 cm^{-1}) and Raman (0–4000 cm^{-1}) spectroscopy. This study provides a comprehensive comparison of these complementary techniques. The resulting data have been used to assign all but a few of the fundamental vibrational modes in the complex. Significant findings in this regard are anomalously low methyl C–H stretching frequencies (2983 and 2910 cm^{-1}), a significantly revised assignment for the manganese–methyl stretch (416 cm^{-1}), and a tentative assignment for the methyl torsion frequency (174 cm^{-1}). A preliminary single-crystal X-ray diffraction study of the complex was also undertaken (*Pcmn*, a = 6.366 (2) Å, b = 11.151 (3) Å, c = 11.955 (3) Å, Z = 4), but a near statistical disorder of the methyl group over all six of the octahedral coordination sites about the manganese precluded derivation of any significant bonding parameters. Prospects for the application of IINS to molecular spectroscopy and to the study of heterogeneous catalytic processes are discussed.

The homogeneous catalysis of organic reactions is often dependent upon the formation of σ bonds between a transition metal and organic alkyl groups. Pentacarbonylmethylmanganese, $Mn(CO)_5CH_3$[2] (**1**), contains one of the first, simplest, and best

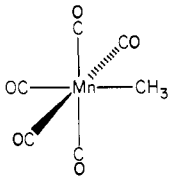

1

known examples of this bonding interaction. It is therefore surprising to find that there are considerable ambiguities concerning the structure, bonding, and vibrational motions of this well-studied molecule. For example, no single-crystal X-ray or neutron diffraction study has been reported. Structural data are limited to a few averaged bond distances and angles determined by the less accurate technique of gas-phase electron diffraction.[3] Vibrational data are more complete, but despite several infrared investigations,[4-7] a number of vibrational assignments are still open to question. In particular, the attribution[5] of the Mn–CH_3 stretch to a band 100 cm^{-1} higher in energy than any of the Mn–CO stretches runs counter to expectations based on the longer Mn–CH_3 distance (2.19 Å) vs. Mn–CO distances (1.86 Å).[3] The issue is further confused by the finding that the Mn–CH_3 bond in $Mn(CO)_5CH_3$ is stronger than the Mn–CO bonds.[8] Other reported anomalies are a strikingly large methyl rotational barrier (11 kJ/mol)[6] and a high geminal J_{H-D} NMR coupling constant in the monodeuterio analogue $Mn(CO)_5CH_2D$.[9]

We have recently completed an extensive series of X-ray, infrared, Raman, and inelastic incoherent neutron scattering (IINS) measurements on $Mn(CO)_5CH_3$ designed to provide a more definitive picture of this prototype metal–alkyl complex. Inelastic neutron spectroscopy[10] was included along with the more commonly employed optical methods for two reasons. First, the comparatively large (incoherent) scattering cross section of the proton leads to a substantially enhanced neutron response to hydrogen motions. This, we thought, would be helpful in identifying methyl modes, particularly those that are optically inactive but neutron active such as rotations and torsions. Second, we were interested in evaluating the potential of IINS in investigating heterogeneous catalytic processes.[11] Neutrons are highly penetrating particles and have been suggested as probes in cases where opacity problems make optical techniques difficult to apply.[12] Knowing that limited neutron flux and energy resolution seriously restrict the use of neutrons in molecular studies, we were interested to see how well the dynamics of a moderately complex molecule could be characterized by neutron methods.[13]

Results

A. X-ray Structural Investigation. As noted, the gas-phase structure of $Mn(CO)_5CH_3$ has been investigated by electron diffraction, but the data were not sufficient even to define all the non-hydrogen bond distances and bond angles.[3] Our original intention was to make both X-ray and neutron-diffraction studies of a single crystal to determine accurately all the geometrical parameters of the molecule. A preliminary room-temperature X-ray study showed, however, that the solid phase is almost entirely orientationally disordered. Each of the six octahedral

(1) (a) BNL Chemistry. (b) BNL Physics. (c) Los Alamos Chemistry. (d) Los Alamos Physics.
(2) Closson, R. D.; Kozikowski, J.; Coffield, T. H. *J. Org. Chem.* **1957**, *22*, 598.
(3) Seip, H. M.; Seip, R. *Acta Chem. Scand.* **1970**, *24*, 3431–3433.
(4) Cattrall, R. W.; Clark, R. J. H. *J. Organomet. Chem.* **1966**, *6*, 167–172.
(5) Khan, O.; Bigorgne, M. *C. R. Hebd. Seances Acad. Sci., Ser C* **1968**, *266*, 792–795.
(6) Dempster, A. B.; Powell, D. B.; Sheppard, N. *J. Chem. Soc. A* **1970**, 1129–1133.
(7) (a) Several workers have examined just the C–O stretching region of the infrared: Wilford, J. B.; Stone, F. G. A. *Inorg. Chem.* **1965**, *4*, 389–393. (b) Kaesz, H. D.; Bau, R.; Hendrickson, D.; Smith, J. M. *J. Am. Chem. Soc.* **1967**, *89*, 2884–2851. (c) Cotton, F. A.; Musco, A.; Yagupsky, G. *Inorg. Chem.* **1967**, *6*, 1357–1364.
(8) (a) Connor, J. A. *Top. Curr. Chem.* **1977**, *71*, 71–110. (b) Lalage, D.; Brown, S.; Connor, J. A.; Skinner, H. A. *J. Organomet. Chem.* **1974**, *81*, 403–409. (c) Connor, J. A.; Zafarani-Moattar, M. T.; Bickerton, J.; ElSaied, N. I.; Suradi, S.; Carson, R.; AlTakhin, G.; Skinner, H. A. *Organometallics* **1982**, *1*, 1166–1174.
(9) Duncan, J. D.; Green, J. C.; Green, M. L. H.; McLauchlan, K. A. *Chem. Commun.* **1968**, 721–722; *Discuss. Faraday Soc.* **1969**, *47*, 178–182.
(10) Howard, J.; Waddington, T. C. *Adv. Infrared Raman Spectrosc.* **1980**, *7*, 86–222 and references cited therein.
(11) Kelly, R. D.; Rush, J. J.; Madey, T. E. *Chem. Phys. Lett.* **1979**, *66*, 159–164.
(12) Howard, J.; Waddington, T. C. *Appl. Surf. Sci.* **1978**, *2*, 102–104.
(13) Only a few IINS studies have included reasonably complete individual vibrational mode assignments and comparison with infrared and Raman spectra for "nontrivial" molecules, especially above ~600 cm^{-1}. Representative examples are carboxylic acids,[14a,b] metal carbonylhydrides,[14c] and metal olefin complexes.[14d]
(14) (a) Berney, C. V.; White, J. W. *J. Am. Chem. Soc.* **1977**, *99*, 6878–6880. (b) Collins, M. F.; Haywood, B. C. *J. Chem. Phys.* **1970**, *52*, 5740–5745. (c) White, J. W.; Wright, C. J. *J. Chem. Soc., Faraday Trans. 2* **1972**, *68*, 1423–1433. (d) Howard, J.; Waddington, T. C.; Wright, C. J. *J. Chem. Soc., Faraday Trans. 2* **1977**, *73*, 1768–1787.

0002-7863/83/1505-2262$01.50/0

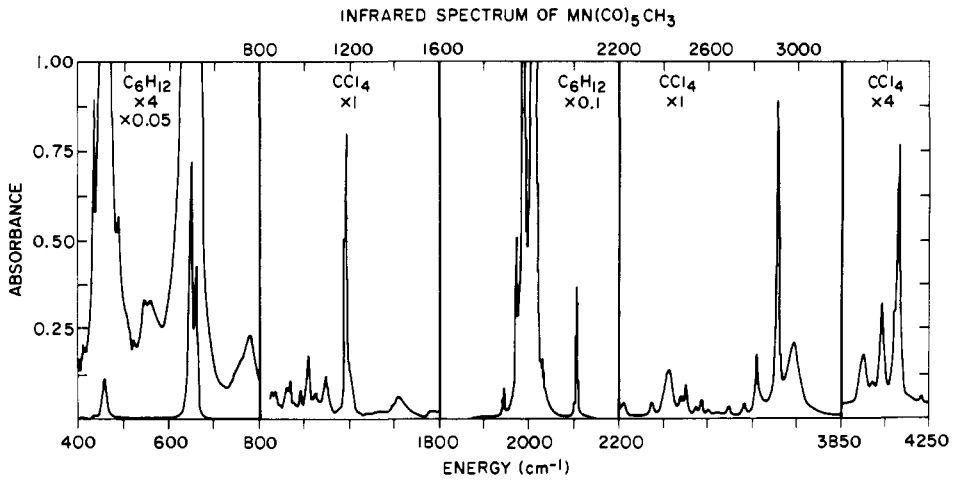

Figure 1. Solution infrared spectra of $Mn(CO)_5CH_3$. Solvent and ordinate expansions for the various spectral regions are indicated on the figure. Spectra of $Mn(CO)_5CD_3$ are shown in Figure 1S.[15]

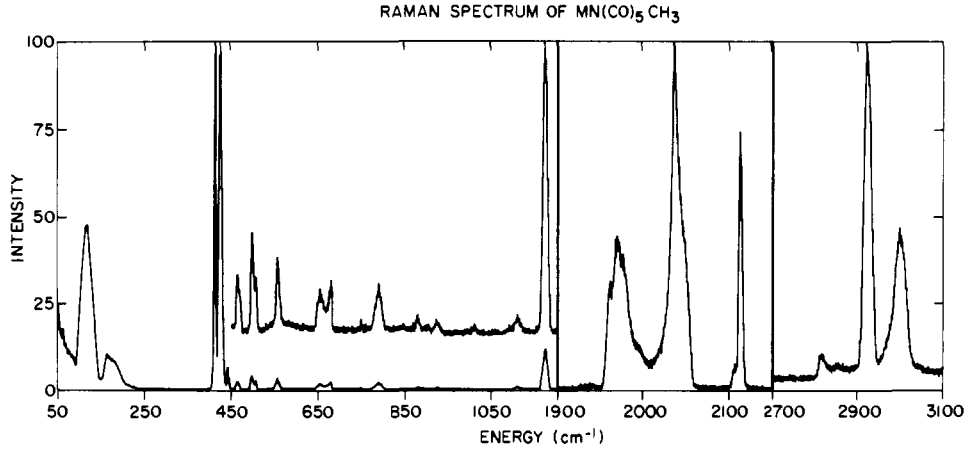

Figure 2. Raman spectrum of solid $Mn(CO)_5CH_3$ at 10 K. The regions 50–1200 and 1900–2300 cm^{-1} were obtained with a 2-cm^{-1} spectral slit width, while the region 2700–3100 cm^{-1} was obtained with 4-cm^{-1} slits. Spectra of $Mn(CO)_5CD_3$ are shown in Figure 2S and comparisons of $Mn(CO)_5CH_3$ and $Mn(CO)_5CD_3$ in Figures 3S and 4S.[15]

coordination sites about the manganese atom was found to be occupied, on average, by about $^5/_6$ of a carbonyl ligand and $^1/_6$ of a methyl ligand. The superimposed methyl and carbonyl carbon atoms could not be resolved; thus, no significant bond distances or angles could be determined. The disorder is confirmed by our Raman measurements (see below) which also show that at least some orientational disorder persists even at 10 K.

B. Infrared and Raman Spectra. Infrared and Raman spectra observed for $Mn(CO)_5CH_3$ and $Mn(CO)_5CD_3$ under a variety of conditions are shown in Figures 1–2 and 1S–4S[15] and summarized in Tables I and IS–IVS.[15] The symmetry classes indicated in Table I are based on the local methyl C_{3v} and $Mn(CO)_5$ C_{4v} geometries. In these point groups, A_1 and E modes would be IR and Raman allowed, B_1 and B_2 modes only Raman allowed, and A_2 both IR and Raman forbidden. The true molecular symmetry, however, is no more than C_s; hence, all modes are *formally* allowed in both the infrared and Raman. In addition, the totally symmetric A_1 modes should be polarized in the Raman. The normal mode assignments indicated in the tables are explained below. Pictorial representations of the corresponding internal symmetry coordinates (cf. $Mn(CO)_5Br$[16]) are shown in Figure 5S.[15]

1. CO Stretching Region (2200–1900 cm^{-1}). The CO stretching region of $Mn(CO)_5CH_3$, $2A_1 + B_1 + E$, has been previously assigned[7] and the same assignment is adopted here. (Weak features observed in the infrared at 2103, 2033, 1976, and 1949 cm^{-1} are assigned to vibrations of the naturally occuring $Mn(^{12}CO)_4(^{13}CO)CH_3$ molecule.[7b,c]) The Raman spectrum of $Mn(CO)_5CH_3$—obtained for the first time in the present work—confirms the assignment of the 2043-cm^{-1} band ($CHCl_3$ solution) as B_1. It should be pointed out that the anomalous depolarization of the 1989-cm^{-1} A_1 band and the weakness of the 2014-cm^{-1} E mode in the Raman spectrum is also seen in $Mn(CO)_5Br$[16,17] and $Fe(CO)_5$.[18] The severely broadened, structured line shape observed for several bands including the ~1970-cm^{-1} A_1 mode in the low-temperature, solid-state Raman spectrum (Figure 2) indicates that a disordered structure (see above) persists down to 10 K. It is interesting to note that the high-energy A_1 equatorial CO stretching vibration at 2114 cm^{-1} (Raman) shifts on deuteration (to 2111 cm^{-1}), indicating mode coupling with the A_1 ν_{C-D} mode at 2125 cm^{-1}. Coupling between these two modes in the deuterated derivative is also supported by the decrease in intensity of the A_1 equatorial CO stretch relative to the other CO stretching modes on deuteration in both the infrared and Raman (Figure 3S).[15]

2. MCO Bending and MC Stretching Region (700–300 cm^{-1}). The δ_{MCO} ($A_1 + A_2 + B_1 + B_2 + 3E$) and ν_{M-C} ($3A_1 + B_1 + E$) region of $Mn(CO)_5CH_3$ has been partially assigned by other workers.[4,5] Our present full analysis shows clearly, however, that the majority of these assignments[5] are incorrect. Our assignments for this region are based in part on the correlation diagram shown in Figure 3 of $Mn(CO)_5CH_3$ with $Mn(CO)_5Br$. Assignments for

(15) Selected figures and tables denoted by the suffix S which appear in the microfilm edition are available as supplementary material.

(16) Ottesen, D. K.; Gray, H. B.; Jones, L. H.; Goldblatt, M. *Inorg. Chem.* **1973**, *12*, 1051–1061.

(17) Edgell, W. F. *Spectrochim. Acta, Part A* **1975**, *31A*, 1623–1640.

(18) Jones, L. H.; McDowell, R. S.; Goldblatt, M.; Swanson, B. I. *J. Chem. Phys.* **1972**, *57*, 2050–2064.

Table I. Observed Frequencies (cm^{-1})[a] for Fundamental Vibrational Modes of $Mn(CO)_5CH_3$ and $Mn(CO)_5CD_3$

idealized assignment	infrared soln[b] room temp CH_3	infrared soln[b] room temp CD_3	Raman soln[c] room temp CH_3	Raman solid room temp CH_3	Raman solid[d] 10 K CH_3	Raman solid[d] 10 K CD_3	IINS solid 10 K CH_3 XM-XA[e]	IINS solid 10 K CH_3 XM-BFD[f]	IINS solid 10 K CH_3 TOF-BFD[g]
				A_1 Block					
$\nu_1:\nu_{CH}^{sym}$	2910[h]	-	-	2919	2925.1	2125.0	-	-	~3050
$\nu_2:\nu_{CO}^{eq}$	2110	2107	2111P	2109.0	2114.0	2111.0	-	-	-
$\nu_3:\nu_{CO}^{ax}$	1989	1989	1989DP	1973 1965	1974 ± 1 1972 ± 1 1964 ± 1	1973 ± 1 1971 ± 1 1963 ± 2	-	-	-
$\nu_4:\delta_{CH_3}^{sym}$	1184	897	-	-	1175.2	889.4	-	1174[i]	1184
$\nu_5:\delta_{MCO}^{eqop}$	662	663	664P	670	679 ± 3	680 ± 2	-	-	-
$\nu_6:\nu_{M-CO}^{ax}$	490	~484	492DP	492.5	493 ± 1	492 ± 1	496[j]	501	508
$\nu_7:\nu_{M-CH_3}$	416 ± 2[h]	399 ± 2[h]	416P	416.5	424.5	402.6	424[j]	424	433
$\nu_8:\nu_{M-CO}^{eq}$	-	-	403P	406.5	412.4	411.2	-	-	-
$\nu_9:\delta_{CMC}^{ax,eq}$[k]	-	-	-	~97	100 ± 2	101 ± 3	~100	-	-
				A_2 Block					
$\nu_{10}:\delta_{MCO}^{eqip}$[k]	(418)[l]	-	-		-	423.7	-	-	-
$\nu_{11}:R_{CH_3}$[k]	-	-	-		174 ± 1	-	~170	-	-
				B_1 Block					
$\nu_{12}:\nu_{CO}^{eq}$	~2043	~2043	2043DP	2034.5	2048 ± 2 2033.0	2047 ± 2 2036.5	-	-	-
$\nu_{13}:\delta_{MCO}^{eqop}$	~608	-	-	-	-	-	-	-	-
$\nu_{14}:\nu_{M-CO}^{eq}$[k]	~506	~508	-	~501	507 ± 1	505 ± 1	-	-	-
$\nu_{15}:\delta_{CMC}^{ax-eq}$[k]	-	-	105DP	~110	115 ± 1	115 ± 1	-	-	-
				B_2 Block					
$\nu_{16}:\delta_{MCO}^{eqip}$[k]	560 ± 2	~560	561P	552	556.5	556 ± 1	-	-	-
$\nu_{17}:\delta_{CMC}^{eqeq}$	-	-	-	-	-	-	-	-	-
				E Block					
$\nu_{18}:\nu_{CH}^{as}$	2983 ± 2[h]	2233	-	2993	3101 ± 2	2246 ± 3	-	-	-
$\nu_{19}:\nu_{CO}^{eq}$	2010	2010	2014DP	1993	1997 ± 3	1995 ± 2	-	-	-
$\nu_{20}:\delta_{CH_3}^{as}$	1420 ± 2[h]	-	-	-	-	-	-	~1435[i]	1456
$\nu_{21}:\rho_{CH_3}$	783 ± 2	587	-	785	789 ± 2	585 ± 1	-	787	789
$\nu_{22}:\delta_{MCO}^{eqip}$	651	663	-	652	656 ± 3	662 ± 1	-	650	~660
$\nu_{23}:\delta_{MCO}^{ax}$	548	538	-	-	-	-	-	550	571
$\nu_{24}:\nu_{M-CO}^{eq}$	458	457	-	459.5	465 ± 1	462 ± 1	-	-	-
$\nu_{25}:\delta_{MCO}^{eqop}$	436	~435	-	436.5	441.7	438.9	-	-	-
$\nu_{26}:\delta_{CMCH_3}$	-	-	153DP	163	162 ± 1	151 ± 2	169	~174	168
$\nu_{27}:\delta_{CMC}^{axeq}$[k]	-	-	-	-	-	-	134	~144	144
$\nu_{28}:\delta_{CMC}^{eqeq}$[k]	-	-	-	-	-	-	115	-	107

[a] 1 meV = 8.07 cm^{-1}. [b] Cyclohexane solution, values ±1 cm^{-1} unless otherwise noted. [c] Chloroform solution, P = polarized, DP = depolarized. [d] Values ±0.5 cm^{-1} unless otherwise noted. [e] Pyrolytic graphite (002) monochromator and analyzer crystals unless otherwise noted. [f] Beryllium (002) monochromator crystal-beryllium filter detector unless otherwise noted. [g] Time of flight with Be filter detector. [h] Carbon tetrachloride solution. [i] Be (110) monochromator crystal. [j] Be (002) monochromator crystal. [k] Tentative assignment. [l] Based on combination band.

the latter molecule were definitively established with the aid of ^{13}C and ^{18}O labeling studies and a full normal coordinate analysis employing a general quadratic valence potential field.[16]

We assign the strong pair of bands observed in the infrared at 662 and 651 cm^{-1} (weak bands at 679 and 656 cm^{-1} in the solid state Raman) to the ν_5 A_1 and ν_{22} E δ_{MCO} modes, respectively. This is opposite to that given in the previous literature.[5] Our identification is confirmed as correct by the polarization of the A_1 solution Raman band at 664 cm^{-1} and by the shift to *higher* energy of the ν_{22} E mode on deuteration. (In the solution infrared of $Mn(CO)_5CD_3$, this shift results in a single, symmetric band at 663 cm^{-1} due to coincidental overlap of the A_1 and E modes.) The shift of the ν_{22} E mode to higher energy on deuteration is a result of coupling between ν_{22} and the ν_{21} E methyl rock which occurs above ν_{22} at 783 cm^{-1} (IR) in $Mn(CO)_5CH_3$ (see below) but below ν_{22} at 587 cm^{-1} in $Mn(CO)_5CD_3$.

The weak infrared shoulder near 608 cm^{-1} is assigned to the remaining high-energy δ_{MCO} mode ν_{13} of B_1 symmetry while the weak pair of IR bands at 560 and 548 cm^{-1} are assigned as the mid-energy B_2 and E symmetry δ_{MCO} modes ν_{16} and ν_{23}, respectively. Of these three modes, only the B_2 is observed in the Raman.[19] The crossover in the correlation of the B_2 and E modes between $Mn(CO)_5Br$ and $Mn(CO)_5CH_3$ may be a result of coupling of the ν_{23} E mode with the methyl rock ν_{21} E mode. As

(19) The Raman band at 561 cm^{-1} appeared to be polarized, though this is not certain due to its weakness. If so, it must be a combination or overtone band, rather than the B_2 fundamental.

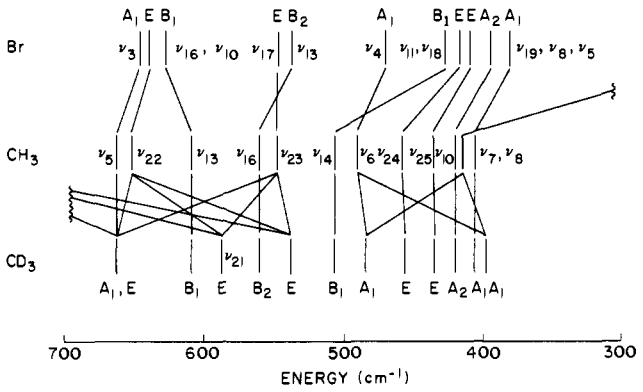

Figure 3. Correlation diagram of the mid-infrared region of $Mn(CO)_5Br$, $Mn(CO)_5CH_3$, and $Mn(CO)_5CD_3$. Mode assignments for $Mn(CO)_5Br$ are from ref 16.

predicted by this argument, the 548-cm^{-1} ν_{23} mode shifts 10 cm^{-1} further to lower energy on deuteration due to stronger coupling with the deuteriomethyl rock at 587 cm^{-1}.

The remaining optically allowed δ_{MCO} mode, ν_{25} (E symmetry), is assigned to the deuterium-sensitive, medium-weak peak observed in the infrared at 436 cm^{-1} (441.7 cm^{-1} in solid-state Raman), analogous to that seen in $Mn(CO)_5Br$.[16] Misassignment of this band in the previous literature[5] is not surprising since it is the only allowed δ_{M-CO} mode to appear in the ν_{MC} region. The only other δ_{MCO} mode, the nominally forbidden A_2 symmetry ν_{10}, would be expected to occur near 420 cm^{-1} based on the correlation with $Mn(CO)_5Br$. A combination band observed at 2428 cm^{-1} (see below) requiring a frequency of ~418 cm^{-1} for ν_{10} is consistent with this hypothesis,[20] as is the appearance of a weak residual peak at 424 cm^{-1} in the Raman spectrum of $Mn(CO)_5CD_3$.

Turning to the metal–carbon stretching region of the infrared spectrum of $Mn(CO)_5CH_3$, we note that it is dominated by a peak at 458 cm^{-1} in the IR which can be readily assigned by comparison with $Mn(CO)_5Br$ to the E symmetry mode ν_{24}. In contrast, the Raman spectrum in this region shows two strong, polarized A_1 bands at 416 and 403 cm^{-1} (CCl_4 solution). In the solid state these occur at 417 and 407 cm^{-1} in $Mn(CO)_5CH_3$ and at 398 and 407 cm^{-1} in $Mn(CO)_5CD_3$ (both at 300 K). Infrared spectra of the hydride and deuteride show only one very weak peak each at 416 and 398 cm^{-1}, respectively, indicating that the ~407-cm^{-1} peak is not sensitive to deuteration. This leads us to conclude that the shifting band near 417 cm^{-1} is the manganese–methyl stretch ν_7 and the fixed 407-cm^{-1} band is the equatorial metal–carbonyl carbon stretch ν_8. The literature assignment[5] of the manganese–methyl stretch to the deuterium insensitive peak at ~560 cm^{-1} is therefore clearly in error by almost 150 cm^{-1}. The remaining A_1 ν_{M-CO} mode ν_6 can be identified by its correlation with the isolated ν_4 A_1 mode of $Mn(CO)_5Br$ as the infrared peak at 490 cm^{-1} (484 cm^{-1} in $Mn(CO)_5CD_3$). This band is not polarized in the Raman spectrum, presumably for the same reason as its A_1 ν_{CO} counterpart ν_3 (see above). Since ν_6 and ν_7 involve collinear oscillators, their coupling is, as expected, much greater than the coupling of the perpendicular oscillators ν_7 and ν_8.

The weak shoulder at ~506 cm^{-1} observed in both the IR and Raman spectra of $Mn(CO)_5CH_3$ can be assigned to the only remaining ν_{M-CO} mode, ν_{14} of B_1 symmetry. This identification requires a rather large shift in position from the corresponding mode in $Mn(CO)_5Br$ but is supported by the observation of combination bands at 2556 and 937 cm^{-1}. Alternatively, the peak at ~506 cm^{-1} could be assigned to a combination mode such as $\nu_7 + \nu_9$.

The correlation presented here of $Mn(CO)_5Br$ with $Mn(CO)_5CH_3$ in the mid-IR region can be easily extended to include $Mn(CO)_5H$.[21] Such an extension confirms the revised assignments for $Mn(CO)_5H$ deduced from inelastic neutron scattering measurements.[14c]

3. Carbon–Metal–Carbon Bending Region (200–50 cm^{-1}). It is generally difficult to make definitive assignments in the δ_{CMC} region of metal carbonyl complexes (cf. $Mn(CO)_5Br$[16]). In the present case there are six expected vibrational modes in this region ($A_1 + B_1 + B_2 + 3E$). The solution Raman spectrum shows a depolarized band at 153 cm^{-1}, which is a distinct doublet (174 and 162 cm^{-1}) in the low-temperature solid-state spectrum. On deuteration the doublet becomes a singlet at 151 cm^{-1}. This indicates that at least one of the two components of the ~170 cm^{-1} doublet in $Mn(CO)_5CH_3$ is the E symmetry methyl–manganese–carbonyl bending mode ν_{26}. Additional, deuterium insensitive bands are observed as a broad asymmetric feature at 115 cm^{-1} with a shoulder at ~100 cm^{-1}. Further arguments concerning assignments for this region are presented with the results of the IINS experiments.

4. Internal Methyl Vibrations. The symmetric and asymmetric C–H stretching modes of $Mn(CO)_5CH_3$ are observed in the infrared at 2910 cm^{-1} (ν_1, in Fermi resonance with $2\nu_{20}$ which appears at 2817 cm^{-1}) and at 2983 cm^{-1} (ν_{18}), respectively. These shift to 2125 and 2233 cm^{-1} on deuteration. Similar features are observed in the Raman spectra. The asymmetric methyl deformation ν_{20} is, as previously noted,[6] weak but is attributed to an infrared peak at 1420 cm^{-1}. In $Mn(CO)_5CD_3$ this mode falls in the δ_{MCO}/ν_{MC} overtone and combination region, probably at 1035 cm^{-1}, though a definitive assignment was not possible. Further evidence supporting the assignment of ν_{20} to the band at 1420 cm^{-1} comes from the IINS spectra (see below). The symmetric methyl deformation, ν_4, appears as a moderately strong infrared and Raman band at 1184 and 1175 cm^{-1}, respectively, which shifts to 898 and 889 cm^{-1} on deuteration. We assign the methyl rock, ν_{21}, to weak infrared and Raman peaks at 783 and 789 cm^{-1}, respectively. On deuteration these shift to 587 and 589 cm^{-1}, due to coupling with ν_{22} (see above). Assignment of the forbidden A_2 methyl torsion will be discussed later.

5. CO Overtone Region (4250–3950 cm^{-1}). Assignments for the ν_{CO} overtone and combination spectrum of $Mn(CO)_5CH_3$ have been made previously.[7c] Our assignments (Table IS)[15] are in agreement with the literature except for the medium intensity band at 4036 cm^{-1} which is assigned to the combination mode $\nu_{12} + \nu_{19}$, not the overtone mode $2\nu_{19}$. Our reasons for making this change are identical with those used by other workers to revise the ν_{CO} overtone and combination assignments for $Mn(CO)_5X$ (X = Cl, Br, I).[22]

6. The Region 3050–2350 cm^{-1}. Residual peaks near 2950 cm^{-1} in the IR spectrum of $Mn(CO)_5CD_3$ were previously noted.[6] We assign these to the ternary combination bands $\nu_2 + 2\nu_{24}$ (3015 cm^{-1}) and $\nu_3 + 2\nu_6$ (2953 cm^{-1}) (Table IIS).[15] Additional bands observed between 2775 and 2375 cm^{-1} can be assigned to 15 or so of the 48 possible binary combinations of ν_{CO} with δ_{MCO} or ν_{M-C} (34 of which are infrared allowed). Shifts observed on deuteration help confirm our assignments and/or make it possible to select among alternate possibilities. Corresponding modes in $Mn(CO)_5Br$ were also generally observable.[16]

7. The Region 1325–800 cm^{-1}. A large number of weak bands are observed in this region. Most of these can be reasonably attributed to overtone and combination bands involving δ_{MCO} and/or ν_{M-C} (Table IIIS).[15] Again, many of the modes observed were also observed in $Mn(CO)_5Br$.[16]

C. Inelastic Neutron Scattering Spectra. We will not attempt to discuss neutron scattering methods here since detailed descriptions are available in the literature.[10] Suffice it to say that IINS spectra are dominated by vibrations involving hyrogen atoms due to the high incoherent neutron scattering cross section of ^1H and the large amplitudes of motion inherent in low-mass hydrogen oscillators. Three types of vibrations in $Mn(CO)_5CH_3$ involve hydrogen motion and are therefore expected to have significant intensity in the IINS. First, there are direct hydrogen vibrations,

(20) The corresponding combination band was observed in $Mn(CO)_5Br$[16] and used to assign the unobserved A_2 mode.

(21) Edgell, W. F.; Fisher, J. W.; Asato, G.; Risen, W. M. *Inorg. Chem.* **1969**, *8*, 1103–1108.

(22) Edgar, K.; Lewis, J.; Manning, A. R.; Miller, J. R. *J. Chem. Soc. A* **1968**, 1217–1221.

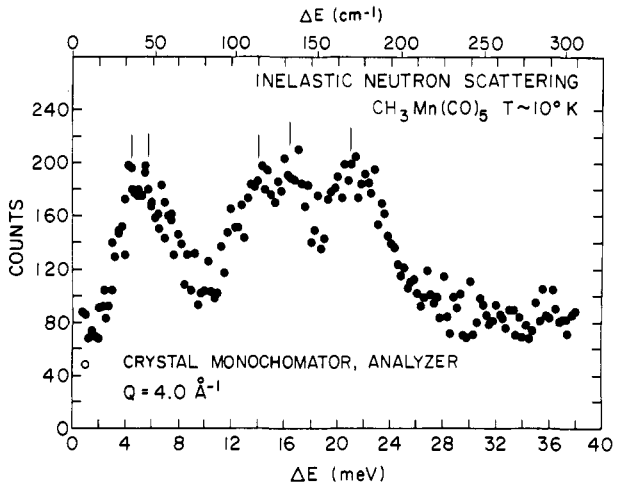

Figure 4. IINS spectrum of solid $Mn(CO)_5CH_3$ at 10 K taken at BNL, using pyrolytic graphite (002) for both monochromator and analyzer crystals. Higher energy data are plotted in Figures 6S and 7S.

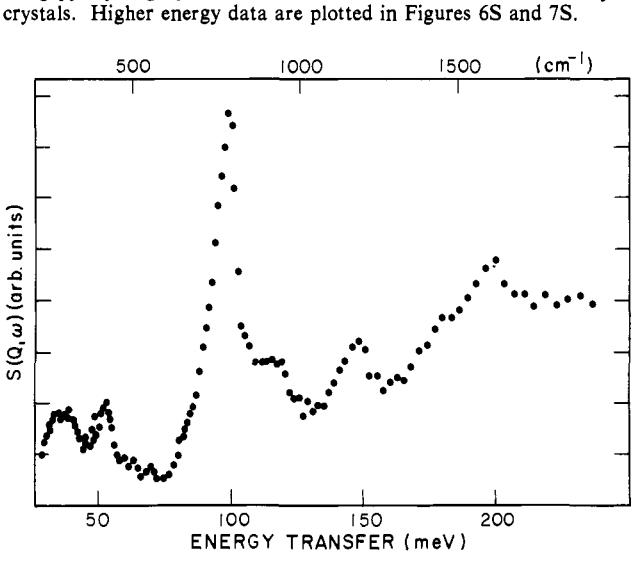

Figure 5. IINS spectrum of solid $Mn(CO)_5CH_3$ at 10 K taken at LANL. Low-energy and high-energy regions are plotted in Figures 8S and 9S.

i.e., those internal to the methyl group. Second, there are indirect hydrogen vibrations resulting from motions of the methyl group as a whole. Finally, there are other normal modes that acquire hydrogen motion via coupling with the above direct and indirect hydrogen vibrations.

The IINS spectra obtained for $Mn(CO)_5CH_3$ are illustrated in Figures 4 and 5 and 6S–9S[15] and summarized in Table I. Considering first direct hydrogen vibrations, the internal methyl modes include the symmetric and asymmetric C–H stretches and deformations ν_1, ν_{18}, ν_4, and ν_{20}, respectively, the methyl rock ν_{21} and the methyl torsion ν_{11}. The resolution problems of IINS are most severe at high energies, hence the C–H stretches appear as a single broad hump at ~3000 cm^{-1} (Figure 9S). Almost all other hydrogen vibrations, however, occur below ~1500 cm^{-1}, where we find that the IINS resolution is sufficient to allow specific identifications to be made. Thus the asymmetric and symmetric methyl deformations are recognizable as weak and medium intensity peaks at 1435 and 1174 cm^{-1} in the BNL IINS spectrum (Figure 7S) (a shoulder at 1456 and a peak at 1184 cm^{-1} in the LANL spectrum, Figure 5[23]). Normally, the nondegenerate symmetric A_1 mode should be only half as intense as the doubly degenerate asymmetric E mode.[10,24] We suspect that the anomalously large area found for the A_1 1174-cm^{-1} peak may be due to coupling with the manganese–methyl stretch (see below).

The methyl rock at ~785 cm^{-1}, a mere bump in the base line in the infrared or Raman, is the dominant peak in the whole IINS spectrum of $Mn(CO)_5CH_3$ (Figure 5 and 7S–9S). The tremendous contrast in the intensities of this mode in the IINS vs. infrared and Raman is an excellent illustration of the complementarity of these techniques.

Methyl torsion modes, such as ν_{11}, are also normally quite intense features of IINS spectra. We were therefore somewhat surprised to find that there were no IINS peaks obviously attributable to this remaining internal methyl vibrational mode. Our analysis of this observation is presented in the Discussion section.

Indirect hydrogen vibrations involving motions of the whole methyl group were also found to be significant features of the IINS spectra. The most obvious example is the methyl–metal–carbonyl bending mode ν_{26} assigned to a frequency of ~170 cm^{-1} by deuteration shifts in the Raman (see above). The IINS spectrum in this region (Figure 4) shows two main peaks at 169 and 125 cm^{-1}. With the aid of a DuPont curve resolver, the broad peak at 125 cm^{-1} can be deconvoluted to give two peaks at 134 and 115 cm^{-1}, with possible evidence for additional structure at ~100 cm^{-1}. The 169-cm^{-1} peak is assigned to the E symmetry ν_{26} mode observed in the Raman. The high intensity of this peak in the IINS is due to a large hydrogen vibrational amplitude resulting from the weak force constant and long lever arm. The 134- and 115-cm^{-1} peaks are attributed to the other two E symmetry C–M–C bending modes ν_{27} and ν_{28}. Nominally these vibrations do not involve hydrogen, but they have the proper symmetry to couple with ν_{26} leading to the second type of indirect hydrogen motions detectable by IINS. A unique aspect of IINS is that the degree of mixing can (in theory) be determined directly from the relative intensities of the peaks involved.[10] The estimated relative intensities (determined by deconvolution and corrected for frequency dependence of the scattering cross section[10]) of the three peaks (roughly 3:1:6 for the 115-, 134-, and 169-cm^{-1} bands, respectively) would suggest that the modes are significantly coupled. This is consistent with results of the normal coordinate analysis of $Mn(CO)_5Br$ which showed extensive coupling of the corresponding low-energy E modes in that complex. The 134-cm^{-1} IINS band is not observed in the Raman (cf. the generally weak intensity of all E modes in the Raman spectrum of $Mn(CO)_5CH_3$). A Raman band is observed at 115 cm^{-1} but it is not sensitive to deuteration and is therefore attributed to the ν_{15} B_1 (or possibly ν_{17} B_2, but cf. the generally greater intensity of B_1 over B_2 modes in this complex) δ_{CMC} mode. The Raman shoulder at ~100 cm^{-1} (IINS shoulder at ~100 cm^{-1}) is attributed to the ν_9 A_1 δ_{CMC} mode. This mode could gain IINS intensity by coupling with the manganese–methyl stretch. Such coupling is not unreasonable since δ_{CMC} and ν_{M-C} modes are found to be coupled in $Mn(CO)_5Br$.[16]

The other fundamental vibration in $Mn(CO)_5CH_3$ observed in the IINS is the manganese–methyl stretch ν_7 assigned—by analogy to the optical spectra—to the medium-weak peak at 424 cm^{-1} (Figures 5 and 6S–8S). This mode is relatively weak in the IINS, possibly due to coupling with the symmetric methyl deformation ν_4 at 1174 cm^{-1}. In-phase coupling of the $Mn–CH_3$ stretch ν_7 with the symmetric methyl deformation ν_4 would increase hydrogen motion in ν_4 as observed (see above), while out-of-phase coupling would decrease hydrogen motion in ν_7. Significant coupling between these two modes is also supported by the unusually high intensity of the $Mn–CH_3$ stretch in the Raman, which upon deuteration decreases in intensity. The methyl deformation correspondingly increases in intensity in the Raman on deuteration consistent with stronger mode coupling. The weak IINS peak at 496 cm^{-1} is attributed to ν_6 (the axial metal–carbonyl carbon stretch) which deuteration studies in the IR and Raman show is coupled to ν_7. It is significant that the other A_1 symmetry modes in this region (ν_5 at 679 cm^{-1} and ν_8 at 412 cm^{-1}) are not present

(23) The frequency discrepancy between the optical and LANL neutron data at high energies is believed to result from the short incident vs. final flight time which leads to frequency calibration errors. The BNL neutron data are in somewhat better agreement with the optical data due to the different experimental technique.

(24) White, J. W.; Wright, C. J. *J. Chem. Soc., Faraday Trans. 2* **1972**, *68*, 1414–1422.

in the IINS, consistent with their observed insensitivity to deuteration in the IR and Raman spectra. We originally attributed the weak IINS peaks at 550 and 650 cm^{-1} (Figures 6S–8S) to these other two A_1 modes. At that time these identifications appeared reasonable since they were nearly compatible with the earlier (incorrect) literature assignments.[5] Our subsequent IR and Raman results, however, clearly show that the IINS peaks at 550 and 650 cm^{-1} are in fact the deuterium-sensitive E symmetry δ_{MCO} modes ν_{23} and ν_{22} which gain intensity by coupling with the strongly IINS-active methyl rocking mode at 787 cm^{-1}.

The strong IINS features (Figure 4) at 46 and 34 cm^{-1} (51 ± 2, 36.5, and 27.5 cm^{-1} in the low-temperature solid-state Raman spectra) are most likely lattice (phonon) modes involving motion of the whole $Mn(CO)_5CH_3$ molecule. The negligible shift on deuteration in the Raman is a result of the small change in oscillator mass (210 vs. 213 amu) implicit in phonon modes.

All of the remaining significant IINS features can be assigned to overtone and combination bands, modes which are much less "forbidden" in IINS than in IR and Raman spectroscopy. Thus, the weak feature near 300 cm^{-1} (Figure 5) corresponds to overtones and combinations of the strong IINS vibrations at ~150 cm^{-1}. A particularly clear-cut example of an IINS combination band is the medium-intensity peak at 941 cm^{-1} (Figure 5, 960 cm^{-1} in Figure 7S) assigned to ν_{21} (ρ_{CH_3}, 787 cm^{-1}) plus ν_{26} (δ_{CMC}, 169 cm^{-1}). An overtone is readily apparent at ~1600 cm^{-1} ($2\rho_{CH_3}$) even though this feature occurs at the upper limit of the energy range currently accessible at the BNL reactor. Finally, a peak which appears in the high-energy Los Alamos data at ~2030 cm^{-1} (Figure 9S) could be due to a combination of the methyl rock and the symmetric methyl deformation.

Discussion

Originally, we had planned to make an extended series of X-ray and neutron diffraction studies of $Mn(CO)_5CH_3$ to obtain a more precise understanding of the structure of the molecule and, in particular, of the metal–methyl bond, which is of special interest. Unfortunately, the orientational disorder of the solid phase defeated our efforts to improve on the existing gas-phase electron diffraction data.

Our vibrational investigations turned out to be more rewarding. In all but a few cases the significantly revised vibrational mode assignments for $Mn(CO)_5CH_3$ given in Table I are believed to be definitive. The exceptions (designated as tentative) are primarily the C–M–C deformations below ~150 cm^{-1}. There are three findings worthy of further discussion: (a) the Mn–CH_3 stretching frequency, (b) the anomalously low C–H stretching frequencies, and (c) the ambiguity in the methyl rotation/torsion assignment. These are all related to the nature of the manganese–methyl bond for which the previous literature posed some puzzling observations.

Consider first, the relative strengths of the Mn–CH_3 and Mn–CO bonds. Unfortunately, there are many different measures of bond strength. Both lengths and bond stretching force constants (or more explicitly their inverse—compliance constants[25]) are often used as related though not identical measures of bond strength. Our revised assignments show that the Mn–CH_3 stretch occurs at a lower frequency (416 cm^{-1}), not a higher frequency (562 cm^{-1}),[5] than most of the Mn–CO stretches (406–506 cm^{-1}). Together with the lower CH_3 vs. CO oscillator mass, this implies a weaker force constant for the Mn–CH_3 vs. Mn–CO stretch. This result resolves the previous discrepancy with the electron diffraction finding that the equilibrium Mn–CH_3 bond distance is 0.3–0.4 Å longer than the Mn–CO bonds.[3] Stretching force constants measure the curvature of a bond's potential energy surface near the equilibrium bond distance. Therefore, stretching force constants and equilibrium bond distances only provide a measure of bond strength near the bottom of the potential energy well. Such measures of bond strength may or may not correspond to either bond dissocation energies (depth of the potential energy well associated with bond) or bond enthalpies (the contribution of each bond in a molecule to the total enthalpy of formation of the molecule). Of the two, bond dissociation energies are more nearly correlated with stretching force constants, but the Mn–CO bond dissociation energy in $Mn(CO)_5CH_3$ does not appear to be known. (The Mn–CH_3 bond dissociation energy in $Mn(CO)_5CH_3$ has been determined to be 153 ± 5 kJ/mol.[8c]) Exact values for the Mn–CH_3 and Mn–CO bond enthalpies depend on the assumptions made but are about 110 and 100 kJ/mol, respectively.[8a] This leads to the interesting conclusion that the relative strengths of the Mn–CH_3 and Mn–CO bonds depends on the type of measurement employed—a well-known but often overlooked fact.

A second aspect of the Mn–CH_3 bond is the form of the bonding interactions. In addition to the obvious σ bond present, there is a proposal that π back-bonding may occur from filled metal d orbitals into methyl C–H antibonding σ^* orbitals. This hypothesis (reverse hyperconjugation) was suggested to explain the high geminal J_{HD} NMR coupling constant in $Mn(CO)_5CH_2D$.[9] Reverse hyperconjugation is well-known in perfluoroalkylmetal complexes and leads to lowering of the asymmetric C–F stretching frequency in $Mn(CO)_5CF_3$ by 150 cm^{-1}.[26] We observe a similar but smaller effect in $Mn(CO)_5CH_3$ (due to the lower electronegativity of H vs. F). In many CH_3X compounds, the five methyl vibrations (mass and Fermi resonance corrected as necessary) are linearly related to the (mass corrected) H–X stretching frequency of the corresponding HX compound.[27] Plots of this relationship for X = F, Cl, Br, I, and $Mn(CO)_5$[28] show that lines drawn through the points for the methyl halides predict the methyl vibrations of $Mn(CO)_5CH_3$ to within ~20 cm^{-1} except for the C–H stretching frequencies. The latter appear at about 100 and 75 cm^{-1} lower energy than expected for the E and A_1 symmetry C–H stretches, respectively. It is not obvious why both the E and A_1 C–H stretches are lowered in $Mn(CO)_5CH_3$ but only the E C–F stretch in $Mn(CO)_5CF_3$. The filled metal d orbitals are of B_2 and E symmetry while the C–X σ^* orbitals in $Mn(CO)_5CX_3$ are of A_1 and E symmetries; hence, only the E symmetry C–X stretch would be expected to be affected by metal-to-σ^* π back-bonding as observed in $Mn(CO)_5CF_3$. In the true molecular symmetry of C_s, the E components are split into A' and A'' allowing for interaction with all of the σ^* orbitals and providing—in theory—a mechanism for lowering both the A and E C–X stretching modes. There appears to be no good reason, however, for a greater symmetry breakdown in $Mn(CO)_5CH_3$ than in $Mn(CO)_5CF_3$. It seems more probable that the A_1 symmetry C–H stretch is lowered in $Mn(CO)_5CH_3$ by σ donation from the more electron-rich C–H (relative to C–F) σ bonding orbital of A_1 symmetry into empty metal p_z and/or d_{z^2} or carbonyl π^* A_1 symmetry orbitals (normal hyperconjugation).[29]

The third aspect of the Mn–CH_3 bond concerns the barrier to rotation. The literature barrier of 11 ± 2 kJ/mol was derived from temperature broadening of the asymmetric C–H stretch.[6] Such a barrier would have to result from noncylindrically symmetric (E type) interactions between the $Mn(CO)_5$ and CH_3 fragments. These are small to begin with (the above cited reverse and normal[29] hyperconjugations) and futhermore are of near-cylindrical symmetry due to the 12-fold multiplicity of the rotor. For these reasons, both we[30] and the original authors[6] question the validity or source of the 11 kJ/mol barrier. In principle, the barrier can be more accurately determined from the methyl rotation/torsion mode ν_{11}.[10] This A_2 symmetry vibration was expected from selection rules to be weak or absent in the infrared

(25) Swanson, B. I. *J. Am. Chem. Soc.* **1976**, *98*, 3067–3071.

(26) Cotton, F. A.; Wing, R. M. *J. Organomet. Chem.* **1967**, *9*, 511–517.

(27) Bellamy, L. J.; Williams, R. L. *J. Chem. Soc.* **1956**, 2753–2757.

(28) The H–Mn stretching frequency in $Mn(CO)_5H$ was taken to be 1784 cm^{-1}.[21]

(29) The C–H σ bonding orbitals of E symmetry would also interact with metal d orbitals of E symmetry, but these are filled orbitals and lead to a destabilizing interaction that contributes to the rotational barrier about a metal–methyl bond: Schilling, B. E. R.; Hoffmann, R.; Lichtenberger, D. L. *J. Am. Chem. Soc.* **1979**, *101*, 585–591.

(30) We believe the literature barrier[6] may be too high since the derivation involved the nonrotationally broadened bandwidth of the asymmetric methyl stretch, taken to be that observed in solid $Mn(CO)_5CH_3$ at −140 °C. This observed bandwidth, however, could be artificially broadened by the orientational disorder found in the solid.

and Raman, but its lack of prominence in the IINS spectrum was surprising in view of the fact that neutrons are known to respond strongly to torsional motions. In the limiting case of unhindered methyl rotation in solid $Mn(CO)_5CH_3$, the $J = 0$ to $J = 1$ rotational transition should appear at 5.3 cm^{-1}. A mode at this energy, although close to the intense IINS peak at zero energy transfer, should not have been difficult to identify. None was observed. The other limiting case is that of highly hindered rotation. This would give rise to a torsional mode with energy $n(BV_n)^{1/2}$, where n represents the barrier multiplicity, V_n its height, and B the rotational constant (5.3 cm^{-1}).[10] A reasonable upper limit for a torsional mode of this type would be ~900 cm^{-1} obtained by combining a 12-fold rotor multiplicity with the literature rotational barrier of 11 kJ/mol.[6] The absence of a prominent IINS band below 900 cm^{-1} clearly attributable to the methyl torsion must be due to near coincidence with another IINS feature and/or to a broad line shape. Broadening would be a natural consequence of both variations in the local torsional potential (resulting from the orientational disorder of the solid phase) and splitting of the torsional mode by quantum mechanical tunneling.[10] We believe that the methyl torsion is most reasonably assigned to the Raman peak at 174 cm^{-1}. This would explain the collapse of the Raman doublet at 174/162 cm^{-1} in $Mn(CO)_5CH_3$ to a singlet at 151 cm^{-1} on deuteration since the ν_{11} torsional mode would shift much further than the 162 cm^{-1} ν_{26} methyl–metal–carbonyl bending mode and become obscured by the strong band at 115 cm^{-1}. In the IINS the torsion would then, together with ν_{26}, contribute to the intensity at 169 cm^{-1}. Alternative assignments consistent with the IINS would be ~40 cm^{-1} under the phonon modes or at 787 cm^{-1} in coincidence with the methyl rock. In any case, knowledge of the methyl torsional frequency is not, by itself, sufficient to determine the barrier to methyl rotation since there is a strong dependence on the rotor multiplicity n; the barrier being given by E_t^2/n^2B where E_t is the torsion frequency. For an E_t of 174 cm^{-1}, the calculated barriers range from 0.4–7.5 kJ/mol for 12-fold to 3-fold rotor multiplicities, respectively. The orientationally disordered crystal structure and the absence of a detectable torsion mode in the solution Raman preclude meaningful statements concerning the rotor multiplicity. Furthermore, a 12-fold rotor with a barrier near 0.5 kJ/mol would be subject to substantial tunneling corrections. We conclude that while rotational barriers about sterically crowded metal–alkyl bonds are well-known,[31] an *accurate* determination of a simple transition metal–methyl rotational barrier has yet to be made.[32]

Finally, we would like to turn to consideration of the neutron as a moleculer probe and to its potential in exploring heterogeneous catalytic processes. As is well-known and evident from our data, molecular vibrations involving hydrogen motions are readily detected with neutrons. Selective probing of hydrogen motions can be very useful in making mode assignments and is unquestionably an important advantage of IINS. It is, however, counterbalanced by a serious disadvantage: the much lower flux (and concurrently lower resolution) of IINS vs. infrared and Raman spectroscopy. Even in relatively simple molecules such as the one studied here (which contains only one type of hydrogen atom), the degraded resolution of IINS results in significant band overlaps and leads to ambiguities in determining peak positions and assignments. The ambiguities are further aggravated by the relatively high IINS intensities of overtone and combination bands. It might be argued that better resolution could have been obtained with a neutron spectrometer designed specifically for molecular spectroscopy[10] rather than the general-purpose instruments we used. But even with the best available technology, the gap between the resolution needed to make neutrons directly competitive with photons and that currently attainable appears too large to be bridged. From the viewpoint of molecular spectroscopy neutrons therefore seem destined to remain a special-purpose probe, used primarily for the investigation of optically weak modes (such as torsions) or to study excitations at very low energy (such as transition between levels split by quantum mechanical tunneling) which are not accessible with optical methods.[10]

We believe there is yet another, relatively unexplored, special application of neutron spectroscopy—the study of heterogeneous catalysis systems. In this case the intention is not to identify all specific modes in complex molecules in solution but rather to employ shifts in already identified modes to probe the chemical reactions of simple molecules on optically opaque supports. IINS molecular spectra exhibit prominent features associated with large amplitude motions of hydrogen-containing functional groups present in catalytically important intermediates. Good examples are the methyl rock in $Mn(CO)_5CH_3$ (this work) and the ethylene CH_2 wag in $KPt(C_2H_4)Cl_3$.[14d] It is clear that a significant fraction of these highly neutron-active modes will be sensitive to the surface orientation of molecules and to molecular rearrangements and dissociative processes. Potential applications of inelastic neutron scattering to heterogeneous catalysis thus appear to be well worth pursuing.

Experimental Section

$Mn(CO)_5CH_3$ and $Mn(CO)_5CD_3$ were prepared by treating $Mn_2(CO)_{10}$ with methanolic NaOH followed by CH_3I or CD_3I (99.5% D, Stohler Isotope Chemicals), respectively,[33] and purified by vacuum sublimation. IR and ^1H NMR spectra showed no evidence of any impurities, in particular no $Mn_2(CO)_{10}$ or $Mn(CO)_5COCH_3$.

X-ray Structure Investigation. A roughly equidimensional (0.3 × 0.3 × 0.3 mm) crystal in the shape of a truncated hexagonal prism obtained by sublimation at near ambient conditions was selected for the structural study. Unit cell parameters and crystal symmetry were determined via Weissenberg and diffraction methods; the latter employed 25 centered reflections and graphite-monochromatized Mo $K\alpha$ (λ = 0.71069 Å) radiation. Crystal data from the Enraf-Nonius CAD-4 automated diffractometer are a = 6.366 (2) Å, b = 11.151 (3) Å, c = 11.955 (3) Å, and V = 848.7 Å^3. Systematic absences ($hk0$ for $h + k = 2n + 1$, $0kl$ for $k = 2n + 1$) are consistent with either the $Pcmn$ or $Pc2_1n$ space groups. The calculated density of 1.64 g cm^{-3} (Z = 4) requires C_s molecular symmetry in the former space group but no special symmetry in the latter. The measured density (aqueous $ZnCl_2$) was 1.56 g cm^{-1}. Observed intensities (1759 reflections: $\pm h,\pm k,\pm l$ for $0° < 2\theta < 30°$ and $+h,+k,+l$ for $30° < 2\theta < 54°$) were corrected for Lorentz and polarization effects. Two standard reflections showed no significant intensity changes during data collection. A symmetry-averaged set of 1116 independent reflections was used in the solution and partial refinement of the structure. All non-hydrogen atomic positions were obtained with the aid of Patterson and Fourier syntheses. Fourier maps in both the centric $Pcmn$ and acentric $Pc2_1n$ space groups revealed the presence of six oxygen atoms about the manganese, indicating a disordered methyl group. The disorder is corroborated by both Raman spectra band shapes (see text) and by preliminary least-squares refinement (in space group $Pcmn$, using 669 reflections with $I > 2\sigma$; $R(F^2)$ = 10.0, $R_w(F^2)$ = 14.1). The refinement was terminated at this point since the data revealed a near statistical disorder of the methyl group over all six coordination sites about the manganese atom, precluding the determination of meaningful bond distances and angles.

Optical Spectra. Infrared spectra of $Mn(CO)_5CH_3$ and $Mn(CO)_5CD_3$ were recorded on a Nicolet MX-1 FT IR in cyclohexane and carbon tetrachloride solution with a scan resolution of 1 cm^{-1}.

Raman spectra of $Mn(CO)_5CH_3$ and $Mn(CO)_5CD_3$ were obtained by using a SPEX 1403 double monochromator equipped with PAR photon counting electronics, an RCA 31034A photomultiplier tube, and a Nicolet 1180E data system. Approximately 50 mW of the 4880-Å line of a Spectra Physics 171 Ar^+ ion laser was used for excitation. The samples were vacuum deposited slowly onto a highly polished copper substrate coupled to a Displex (Air Products) closed-cycle helium cryostat. Deposits made at 10 K showed rather broad features characteristic of poor crystallinity. Several attempts were made to obtain more crystalline samples by high-temperature annealing and depositing at higher (>200 K) temperatures. The spectra so obtained, while sharper than those obtained with low-deposition temperatures, still exhibited broad structural features characteristic of high disorder. Spectra obtained at several temperatures in the range 10–300 K were essentially the same; data

(31) See, for example: McCormick, F. B.; Angelici, R. J.; Pickering, R. A.; Wagner, R. E.; Jacobson, R. H. *Inorg. Chem.* **1981**, *20*, 4108–4111 and references therein.

(32) The best measurements of this type to date appear to be by Jordan and Norton: Jordon, R. F.; Norton, J. R. *J. Am. Chem. Soc.* **1979**, *101*, 4853–4858.

(33) King, R. B. "Organometallic Syntheses"; Academic Press: New York, 1965; Vol 1, p 147.

reported here were measured at 300 and 10 K to be consistent with the IINS data. Polarization studies were also made with a saturated $CHCl_3$ solution.

Inelastic Neutron Scattering Spectra. IINS measurements at BNL were carried out at the High Flux Beam Reactor, using a triple-axis spectrometer. Low-energy spectra were obtained with pyrolytic graphite (002) for both monochromator and analyzer crystals and a BF_3 proportional counter detector. Data were measured at a fixed **q** for constant monitor counts. High-energy spectra were obtained with a beryllium (002 and 110) monochromator and a liquid-nitrogen-cooled beryllium filter analyzer (cutoff energy of 5.2 meV and mean band-pass of ~3.5 meV). Substantial gains in counting rates should be possible with a beryllium filter analyzer with a larger solid angle of acceptance. The polycrystalline sample of $Mn(CO)_5CH_3$ (10.6 g) was mounted in a cylindrical aluminum can 1.9 cm in diameter maintained at 9 K. Transmission measurements showed that the sample scattered 75% of the incident neutrons.

A revised sample holder was prepared prior to data collection at Los Alamos to decrease the degree of multiple scattering. A 27.6-g sample of $Mn(CO)_5CH_3$ was mounted in an annular geometry in a cylindrical aluminum can (0.93 in. i.d.) whose center was kept hollow by a second aluminum cylinder (0.625 in. o.d.). The IINS measurements at Los Alamos were then carried out at ~10 K by using the WNR pulsed-spallation neutron source and a beryllium filter analyzer time-of-flight spectrometer. The instrument used in the present experiment is a prototype[34] of a more elaborate version currently under development at the WNR. The incident and final flight paths were 11.42 and 0.26 m, repectively, which, along with the filter band-pass, primarily determine the energy resolution of approximately 12% ($\Delta E/E$) at 150 meV. Three adjacent pie-shaped Be filter sections, each 15 cm long, were centered at 72°, 90°, and 108° scattering angles from the sample. Each of these filter sections was viewed by six ^3He counters and time analyzed separately from each other in order to correct for variations in backgrounds. Frame overlap was eliminated with a gadolinium foil filter. After background subtraction and correction for filter transmission factors, the spectra were divided by the spectrum of incident neutrons and related to the scattering function $S(Q, \omega)$ which is the quantity plotted in the figures.

(34) Eckert, J.; Silver, R. N.; Soper, A. K.; Vergamini, P. S.; Goldstone, J. A.; Larson, A. C.; Seeger, P. A.; Yarnell, J. *Proc. Int. Collab. Adv. Neutron Sources, 4th* **1981** (KENS Report II).

Acknowledgment. We are grateful for the assistance of Dr. Graheme Williams in the X-ray diffraction study of $Mn(CO)_5CH_3$ and to Professors T. Spiro and H. Kaesz for helpful discussions. The work reported here was carried out at the Brookhaven and Los Alamos National Laboratories under contract with the U.S. Department of Energy.

Registry No. $Mn(CO)_5CH_3$, 13601-24-6; $Mn(CO)_5CD_3$, 15653-52-8.

Supplementary Material Available: IR and Raman spectra of $Mn(CO)_5CD_3$ (Figures 1S–4S), IINS spectra of $Mn(CO)_5CH_3$ (Figures 6S–9S), pictoral representations of internal vibrational symmetry coordinates (Figure 5S), and vibrational overtone and combination frequencies for $Mn(CO)_5CH_3$ (Tables IS–IIIS) (20 pages). Ordering information is given on any current masthead page.

X-ray Absorption Spectra of Ruthenium L Edges in $Ru(NH_3)_6Cl_3$

T. K. Sham

Contribution from the Department of Chemistry, Brookhaven National Laboratory, Upton, New York 11973. *Received June 21, 1982*

Abstract: X-ray absorption spectra of ruthenium L edges of $[Ru(NH_3)_6]Cl_3$ have been obtained with synchrotron radiation. It is found that Ru L edges exhibit white lines characteristic of ligand-field and spin–orbit effects. Analysis of the data on the basis of local symmetry and the electronic configuration of the complex yields a $10Dq$ value of 3.93 eV.

Recent advances in synchrotron radiation technology have opened up new avenues for studying X-ray excitation of core electrons into the empty valence levels (discrete bound states) and the continuum.[1-10] In a typical X-ray absorption experiment, the absorption coefficient of a particular edge as a function of the photon energy below and above the ionization threshold is measured. In condensed matter studies transitions from the core level to the valence levels often produce structures at the edge characteristic of the local symmetry and electronic configuration of the atom; transitions to the continuum, on the other hand, give rise to oscillations in the absorption coefficient up to as much as 1000 eV above the threshold. The latter phenomenon is called extended X-ray absorption fine structure (EXAFS) and has been well understood,[1-10] while studies of the near-edge region with synchrotron radiation remain relatively limited.[4,11-14] Recently,

(1) Eisenberger, P.; Kincaid, B. M. *Science (Washington, D.C.)* **1978**, *200*, 1441 and reference therein.
(2) Stern, E. A. *Contemp. Phys.* **1978**, *19*, 289.
(3) Winick, H.; Bienenstock, A. *Annu. Rev. Nucl. Part. Sci.* **1979**, *28*, 33. Watson, R. E.; Perlman, M. L. *Science (Washington, D.C.)* **1978**, *199*, 1295. Kunz, C., Ed. "Synchrotron radiation-techniques and applications" Springer-Verlag: New York, 1979.
(4) Shulman, R. G.; Yafet, Y.; Eisenberger, P.; Blumberg, W. E. *Proc. Natl. Acad. Sci. U.S.A.* **1976**, *73* 1384.
(5) Cramer, S. P.; Hodgsen, K. O.; Stiefel, E. I.; Newton, W. E. *J. Am. Chem. Soc.* **1978**, *100*, 2748. Cramer, S. P. Ph.D. Thesis, Stanford University, 1978.
(6) Brown, M.; Peierls, R. E.; Stern, E. A. *Phys. Rev. B: Solid State* **1977**, *15*, 738.
(7) Citrin, P. H.; Eisenberger, P.; Kincaid, B. M. *Phys. Rev. Lett.* **1976**, *36*, 1346.
(8) Teo, B. K.; Lee, P. A. *J. Am. Chem. Soc.* **1979**, *101*, 2915.
(9) Stern, E. A.; Sayers, D. E.; Lytle, F. W. *Phys. Rev. Lett.* **1976**, *35*, 298.
(10) Brown, F. C.; Backrach, R. Z.; Bianconi, A. *Chem. Phys. Lett.* **1978**, *54*, 425.
(11) Early edge studies carried out before the synchrotron radiation era was documented: Srivastava, U. C. and Nigam, H. L. *Coord. Chem. Rev.* **1972–1973**, *9*, 275. For the advantage of synchrotron radiation over conventional source, see ref 1–3.
(12) Brown (Brown, F. C. *Solid State Phys.* **1974**, *29*, 1) reviewed early synchrotron work of outer edges.

0002-7863/83/1505-2269$01.50/0